# REINFORCED PILED EMBANKMENT FOR A HIGH-SPEED RAILWAY OVER SOFT SOIL: A NUMERICAL AND ANALYTICAL INVESTIGATION

**Yan Zhuang** *(corresponding author)*
Hohai University, Geotechnical Research Institute
Key Laboratory of Ministry of Education for Geomechanics and Embankment Engineering
1 Xi Kang Road, Nanjing210098, China
E-mail: zhuangyan4444@hotmail.com

**Xiaoyan Cui**
Hohai University,
College of Civil and Transportation Engineering
1 Xi Kang Road, Nanjing210098, China
E-mail: cui19890213@126.com

**Keywords**

reinforced piled embankment, high-speed railway, numerical simulation, analytical method

**Abstract**

*A geosynthetic, reinforced, piled embankment is an effective and economic method to solve the problems of possible bearing failure, unacceptable settlement and slope instability for an embankment built over soft soil; this has led to its widespread use, especially for high-speed railway embankments. Some design methods have been developed to assess the performance of these reinforced structures, which are mainly based on the results from small-scale models and numerical simulations. However, the reliability of these methods needs to be validated under full-scale field tests. This paper presents a numerical and analytical study for a full-scale field test of the Fengyang high-speed railway embankment. The results were analyzed and discussed in terms of the settlement of subsoil, the stress-concentration ratio (SCR), the axial force and the frictional stress of the pile. They showed that the settlement of the subsoil, from both the finite-element method (FEM) and the analytical method, were in good agreement with the measurement, and thus was a reliable parameter to assess the performance of the piled embankment with reasonable accuracy. The SCR was overestimated by the modified Terzaghi method, with a difference of 25%, while it was underestimated by the FEM, with a difference of approximately 20%. It was also shown that the tensile force in the reinforcement could be effectively assessed using the proposed analytical method, while it was overestimated by the FEM with a difference of 44%.*

## 1 INTRODUCTION

The high-speed railway is the result of modern science and technology, and an important indicator of railway modernization. The construction of a high-speed railway network in China has been developing rapidly over the past 10 years, for example, the Beijing-Shanghai, Shanghai-Hangzhou, Shanghai-Nanjing, and Wuhan-Guangzhou high-speed railways. The controls of the post-construction settlement and the improvement in construction speed have been the two main technical problems for high-speed railways constructed on soft soil. The piled embankment has been proven to be an interesting solution that prevents the failure or excessive deformation of the embankment compared to the traditional soft-foundation improvement methods for embankments built over soft soils, such as preloading (Magnan, 1994)[1]. The inclusion of a geosynthetic reinforcement enhances the load-transfer mechanism and so minimizes the differential and maximum settlements (Gangakhedkar, 2004) [2].

Many experimental tests, criteria and analytical methods have been proposed to analyze the interactions between the embankment, the geosynthetic reinforcement, the

piles and the subsoil. Terzaghi (1943)[3] assumed that the shearing resistance of the soil during arching was mobilized along two vertical planes through the side of the inclusion, and the considered shear stress on the vertical interfaces originating from the rigid supports on either side of a 'trapdoor', where the support was reduced. Russell and Pierpoint (1997) [4] developed the arching theory proposed by Terzaghi (1943) [3] to take account of the three-dimensional problems of the piled embankments. Hewlett and Randolph (1988) [5] conducted 3D model tests and presented a semi-circular model (in 2D) or a hemispherical dome model (in 3D) to describe the arching, and of the uniform thickness, with no overlap. This method assumed that the pressure acting on the subsoil was uniform and considered the failure condition either at the crown of the arch or the pile cap. The British Standard BS8006-1 (2010) [6] estimated the vertical stress on the top of the piles based on the modified Marston's formula for positively projecting conduits. The magnitudes of the load carried by the piles and the reinforcement were evaluated. The three-dimensional shape analysis developed by Hewlett and Randolph (1988) [5] was also included in BS8006-1 (2010) [6]. However, the effect of the subsoil in the two methods of BS8006-1 (2010) [6] was not considered. The criterion for the German EBGEO (2011) [7] was based on the method proposed by Kempfert et al. (2004) [8]. In this method, the average vertical pressure acting on the columns and the soft foundation soil were calculated by considering hemispherically shaped domes spanning the distance between the pile caps. Van Eekelen et al. (2011) [9] analyzed and modified BS8006-1 (2010) [6] in terms of the calculation method of the tensile force in the tensile reinforcement for the 3D situation. They reported that BS8006-1 (2010) [6] designed a relatively strong and expensive geosynthetic reinforcement in comparison with other design models (e.g., EBGEO, (2011) [7]), and the modified method was better in evaluating the geosynthetic reinforcement than that of the original BS8006-1 (2010) [6], but the geosynthetic reinforcement predicted by EBGEO (2011) [7] was much closer to the FEM results. Zhuang et al. (2014) [10] proposed a simple analytical model for the reinforced-piled embankment to assess the contribution of the reinforcement and the subsoil. The simplified model can be used to estimate the magnitude of the tensile force generated in the reinforcement, the vertical stress increment acting on the subsoil for multi-layered soft soils, the maximum settlement at the surface of the subsoil and the maximum strain of the geosynthetics. The methods illustrated above are either based on the results from small-scale models or the numerical analysis, whose reliability should be validated under full-scale field tests.

Some research has also been conducted based on a numerical simulation, which has the advantage of being able to analyze the interactions between the embankment, the geosynthetic reinforcement, the piles and the soft-soil foundation with reasonable accuracy. Han and Gabr (2002) [11] performed a numerical study of reinforced, piled embankments, including the underlying subsoil. Le Hello and Villard (2009) [12] introduced a numerical and experimental method for a geosynthetic reinforced, piled embankment. Two main mechanisms, including the arching effect and the membrane effect of the geosynthetics, were analyzed. But very limited attention has been paid to a settlement-time relationship, especially a post-construction settlement, which is critical to the performance of pavements, especially a high-speed railway built on embankments.

This paper presents a numerical and analytical study for the field case of the Fengyang high-speed railway. The results are discussed in terms of the stress-concentration ratio (SCR), the development of the settlement of subsoil at the centerline of the embankment, the distribution of the settlement of subsoil along the width of the embankment, the lateral deformation of the subsoil, the axial force and the negative frictional stress along the piles. The purpose of this paper is to compare the results of the numerical simulation and the analytical methods with measurements made on a full-scale field case to assess their accuracy in analyzing the behavior of the reinforced, piled embankment.

## 2 DESCRIPTIONS OF THE FENGYANG HIGH-SPEED RAILWAY CASE STUDY

### 2.1 General project information

The test site of the Fengyang high-speed railway was located in Fengyang County, Anhui Province, China. Details of its construction, the ground conditions, the setup of the tests, the instruments and the measurement results can be obtained from Zeng (2010) [13]. In the present paper, only the information required to describe the numerical simulation and the analytical methods was proposed.

The embankment is 3.6–4.8 m high with a crest width of 13.6 m. The side slope of the embankment is 1V to 1.5H. The thickness of the soft soil ranges from 13.1 to 16.6 m. Below the soft soil is the weathered rock, with a bearing capacity in the range 250 to 800 kPa. The CFG (cement fly-ash gravel) pile-net composite foundation was used in the field case to improve the soft ground. The geosynthetic reinforcement with a tensile stiffness of 1 MN/m in the longitudinal and transverse directions was also used to strengthen the embankment.

The field case of the Fengyang high-speed railway was tested with a total length of 370 m from DK854+640 to DK855+010. The embankment was divided into three sections, with different ground-improvement methods.

In this paper, only the section of DK854+655 (defined as Section A), reinforced by CFG pile-net composite foundation and preloading, was analyzed. The preloading in Section A was about 3 m high with a side slope of 1V to 1H, and was applied to the top of the embankment for approximately 450 days. Detailed information about Section A is summarized in Table 1.

## 2.2 Site conditions

The height of the embankment in Section A was 3.6 m. The fill material consisted mainly of gravel mixed with sand, with an average unit weight of 20 kN/m$^3$. The CFG piles were arranged in a square pattern with a spacing of 1.8 m, and designed with circle pile caps (see Fig. 1(a)).

**Table 1**. General information of Section A for the Fengyang high-speed railway.

| Section A | Embankment height (m) | Pile length (m) | Pile spacing (m) | Pile cap diameter (m) | Cushion structure |
|---|---|---|---|---|---|
| | 3.6 | 10.0 | 1.8 | 1.0 | 0.6 m gravel cushion + a layer of geogrid |

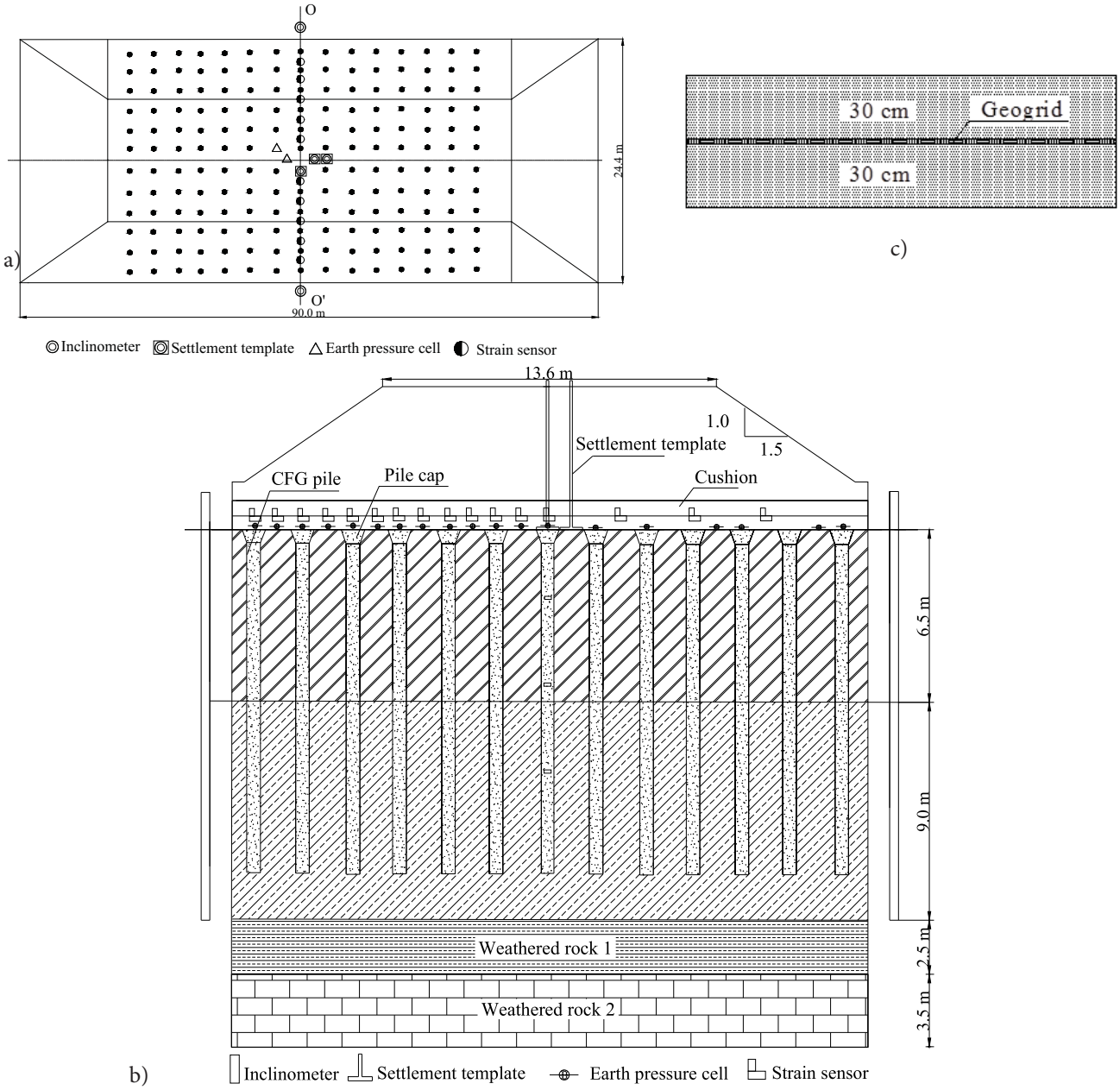


**Figure 1**. Plan view and cross-section of the test embankment in the Fengyang high-speed railway:
a) Plan view of the experimental site at Section A; b) Cross-section of the embankment; c) Structure of the cushion.

Table 1 summarizes the information about the piles. Fig. 1(b) shows the cross-section of the test embankment. It can be seen that two layers of clay were laid below the embankment. The bearing capacity of the first layer of clay was 150 kPa, with a thickness of 6.5 m, while the thickness of the second layer was 9.0 m, with a bearing capacity of 200 kPa. The main properties of the clays are summarized in Table 2. Beneath the clay layers are two layers of weathered rock with a high bearing capacity. One layer of the biaxial geogrid was sandwiched between two, 0.3-m-thick, gravel layers to form a 0.6-m-thick composite-reinforced bearing layer (see Fig. 1(c)).

**Table 2**. Main soil properties of Section A.

| Stratum | Water content (%) | Void ratio | Compression index | Critical shear stress ratio |
|---|---|---|---|---|
| Clay 1 | 25.0 | 0.8 | 0.23 | 0.79 |
| Clay 2 | 22.7 | 0.7 | 0.19 | 1.03 |

### 2.3 Test setup and instruments

As shown in Fig. 1, the earth pressure cells were placed on the top of the pile caps and the surface of the subsoil. Piezometers to measure the pore-water pressures were placed at different depths of the subsoil. The settlement plates were installed on the top of both the pile caps and on the surrounding soils. Strain sensors in the geogrid were installed to measure the strain of the geogrid. The observation started at the beginning of the construction for the embankment in November in 2007 and lasted for about 2 years after it was completed.

The measurements of the field case will be presented and discussed in the following sections to validate the results derived from the numerical simulation and analytical methods, in terms of the vertical stress acting on the pile cap and the subsoil, the settlement and the lateral deformation of the soil, the axial force and the negative frictional stress along the piles.

## 3 NUMERICAL SIMULATION

### 3.1 Description of the numerical model

The finite-element method (FEM), which was carried out using the finite-element package 'ABAQUS' (version 6.12), was used to simulate the field case of the Fengyang high-speed railway. Since the embankment was symmetrical along its centerline, only half of the embankment was modeled for the FEM. The foundation soil was taken to be 21.5 m deep, overlying a rigid impermeable stratum. The horizontal length of the model was taken to be 36.6 m, so that the boundary effect can be minimized. A 1.8-m-wide section with a center row of piles beneath the embankment was selected for the analysis (see Fig. 2(a)), so that a truly full-3D model can be obtained. The 3D numerical model is shown in Fig. 2(b). The water table was at a depth of 0.8 m below ground level, and the initial pore pressures prior to the embankment construction were taken to be hydrostatic. A zero-pore-pressure boundary condition was applied at the level of the water table to model the free drainage, which means that the water is allowed to drain via this plane of the soft clay. The bottom of the model is defined as impermeable, and a lateral flow is not permitted across the vertical planes. With regard to the displacement boundary condition, no displacements in the direction perpendicular to the symmetry planes and to the base were allowed.

The embankment fill was assumed to be dry, granular material, and was modeled with a linear-elastic, perfectly

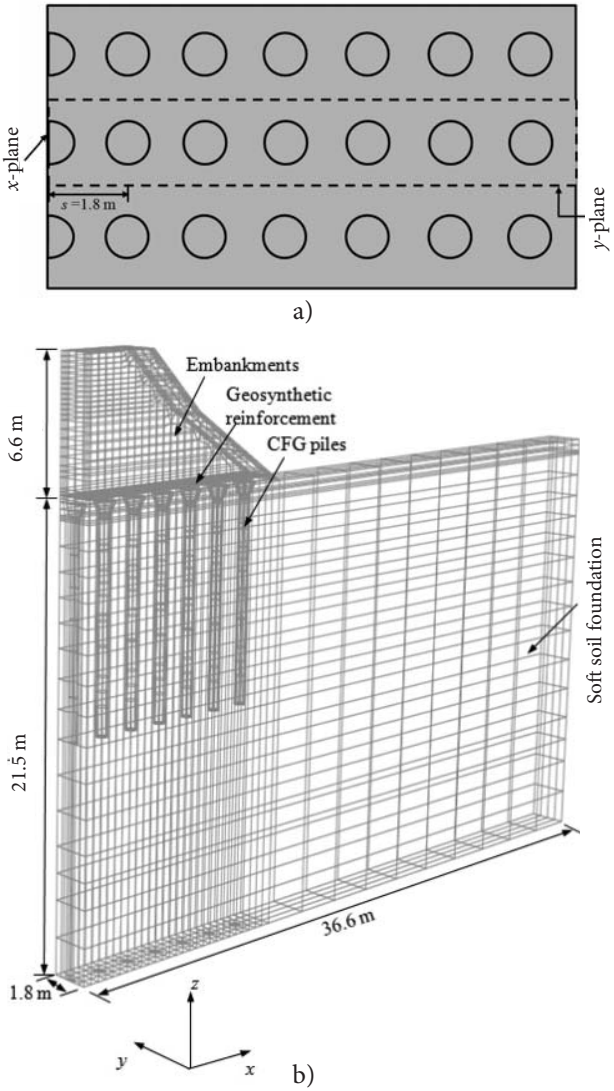


**Figure 2**. Three-dimensional finite-element model of the embankment: (a) Plan view for layout of CFG piles; (b) 3-dimensional finite-element model.

**Table 3**. Summary of the material parameters used in the finite-element analyses.

| Material | $E$ (MPa) | $\gamma$ (kN/m$^3$) | $c$ (kPa) | $\varphi$ (°) | $\nu$ |
|---|---|---|---|---|---|
| Embankment | 60 | 20 | 40.0 | 20.0 | 0.15 |
| Clay 1 | 6.4 | 19 | 37.3 | 20.4 | 0.30 |
| Clay 2 | 9.2 | 20 | 75.6 | 27.3 | 0.30 |
| Weathered rock 1 | 40 | 21 | 63.9 | 19.3 | 0.25 |
| Weathered rock 2 | 80 | 22 | 63.9 | 19.3 | 0.25 |
| CFG pile | 22000 | 23 | | | 0.10 |
| Geosyntheic reinforcement | Tensile stiffness kg = 1.0 MN/m; Poisson's ratio $\nu$ = 0.3 (assumed) | | | | |

plastic model with the Mohr-Coulomb failure criterion, as well as two layers of weathered rocks. The pile and the geogrid were modeled as a linear elastic material. The two clay layers were modeled using a modified cam clay (MCC) model. The parameters used are summarized in Tables 2 and 3. The critical shear stress ratio of the two clay layers (see Table 2) for the MCC model were 0.79 and 1.03, respectively, and with a Poisson's ratio value of 0.3. The compressibility of the subsoil can be quantified by the compression index ($C_c$). In cam clay, the compressibility is represented by the parameters $\lambda$ and $\kappa$. The parameter $\lambda$ is equal to $C_c$ divided by 2.3, and it is assumed in this study that $\kappa$ is equal to 0.1 times $\lambda$. In addition, the initial yield surface size $a_0$, a required input for the MCC model, is computed using the following:

$$a_0 = \frac{1}{2}\exp\left[\left(1+e_0\right)\frac{e_N - e_0\kappa\ln p_0}{\lambda-\kappa}\right] \qquad (1)$$

where $e_0$ is the initial void ratio, $p_0$ is the overburden pressure, $e_N$ is the intercept of the normally consolidated line with a ratio axis in the $e$-ln$p$' plane, $\lambda$ is the slope of the virgin consolidation line, and $\kappa$ is the slope of the swelling line.

The geogrid in the FEM was modeled using 4-node, full-integration, 3-dimensional membrane elements (M3D4). The clay layers below the water table were modeled using 8-node, stress-pore-pressure-coupled, brick elements (C3D8P), while 8-node brick elements (C3D8) were used for the other materials. The interface friction angle between the geogrid and the embankment was assumed to be equal to the friction angle of the embankment fill, which was also assumed in Liu et al. (2007) [14]. According to the equation proposed by Potyondy (1961) [15] for the clay, the interface friction angle ($\varphi_i$) between the pile and the subsoil can be determined as follows:

$$\varphi_i = \left(0.6\text{~}0.8\right)\varphi_s \qquad (2)$$

where $\varphi_s$ is the friction angle of the soil. In this analysis, the ratio of the interface friction angle ($\varphi_i$) and the friction angle of the soil ($\varphi_s$) was assumed to be 0.7. And duplicated nodes were used to form a zero-thickness interface between the pile and its surrounding soil.

## 3.2 Comparison of the numerical results and the measurements

### 3.2.1 Variation of the settlement at the centerline of the embankment

Fig. 3 shows the comparison of the numerical results and the measurements for the settlement of the subsoil at the centerline of the embankment. The settlement of the subsoil increased with an increase of the embankment height. After the construction of the embankment, a few subsequent settlements occurred due to the consolidation of the foundation soil. The results of the settlement calculated using the FEM were similar to the measurements, while they showed a difference after unloading the preloading. The settlement of the subsoil decreased by approximately 4 mm for the FEM, while the change was almost negligible for the measurement. The final settlement of the subsoil derived from the FEM and the measurement was in good agreement, with a slight difference of 8.2%. The settlement of the subsoil at the centerline of the embankment can therefore be evaluated using the FEM with reasonable accuracy.

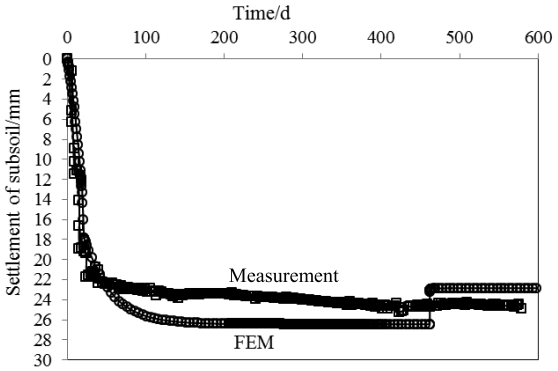


**Figure 3**. Development of the settlement of subsoil at the centerline of the embankment.

### 3.2.2 Settlement of the subsoil along the width of the embankment

The results of the settlement of the subsoil along the width of the embankment from the FEM and the measurement are presented in Fig. 4. The maximum settlement of the subsoil occurred at the centerline of the embankment, and decreased towards the right toe of the embankment. As is clear in Fig. 4, the FEM and the measurement showed a similar profile for the settlement distribution (the curve likely to be parabolic). The settlement of subsoil, from both the FEM and the measurements in the field near

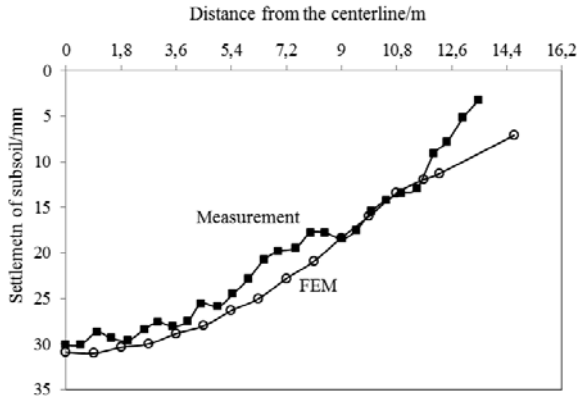


**Figure 4**. Settlement of subsoil along the width of the embankment.

the centerline of embankment, was in good agreement. For the measurements, the settlement at the right toe of the embankment is approximately 10.8% of that at the centerline of the soil surface, while for the FEM, the corresponding percentage is approximately 30.2%. It was concluded that the numerical method overestimated the settlement on the side of the embankment.

### 3.2.3 Lateral deformation of the subsoil

Fig. 5 shows a comparison between the numerical results and the measurement in terms of the lateral deformation near the right toe of the embankment at the end of the construction. As shown in Fig. 5, the measured maximum lateral deformation was 7 mm, and this occurred at the surface of the subsoil, which showed a similar shape to the lateral deformation profile from the FEM. However, the magnitude of the lateral deformation was overestimated, with a difference of 17.6%, which may be due to the use of isotropic homogeneous soil models and soil parameters in the FEM to simulate what were anisotropic and nonhomogeneous soils in the field. Since the piles were founded on weathered rock layers rather than the fully rigid layer, the value of the lateral deformation at the bottom of the piles from the FEM was not equal to zero, which was also different to that of the measurement.

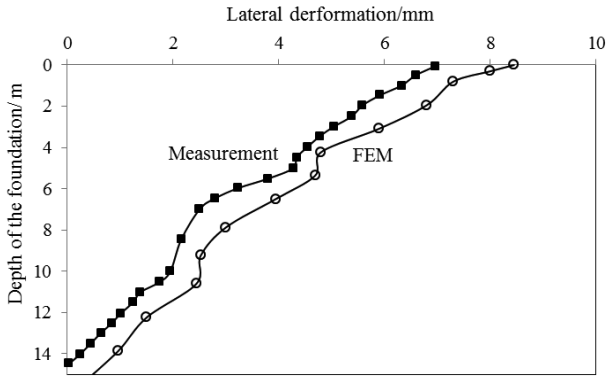


**Figure 5**. Lateral deformations of the subsoil at the right toe of the embankment.

### 3.2.4 The stress-concentration ratio (SCR)

The degree of stress concentration from the soil to the piles is typically evaluated using the stress-concentration ratio (SCR), which is defined as the ratio of the stress on the pile caps to that on the subsoil, and is given by:

$$SCR = \frac{\sigma_p}{\sigma_s} \qquad (3)$$

where $\sigma_p$ is the vertical stress acting on the pile caps, and $\sigma_s$ is the vertical stress acting on the subsoil. The higher the concentration ratio, the more the stress is transferred onto the piles. As is clear in Fig. 6, the value of the SCR was almost linearly increasing with an increase of the embankment height, due to the arching in the embankment, which meant that the vertical stress transferred from the subsoil to the pile caps. The value of the SCR fluctuated after the construction of the embankment for the measurement, which may be due to the consolidation of the subsoil and the influence of the rainy season. The SCR from the FEM reached a stable value after the construction of the embankment, while it decreased after unloading the preloading. It is also clear in Fig. 6 that the SCR was underestimated by the FEM, with a difference of approximately 20%.

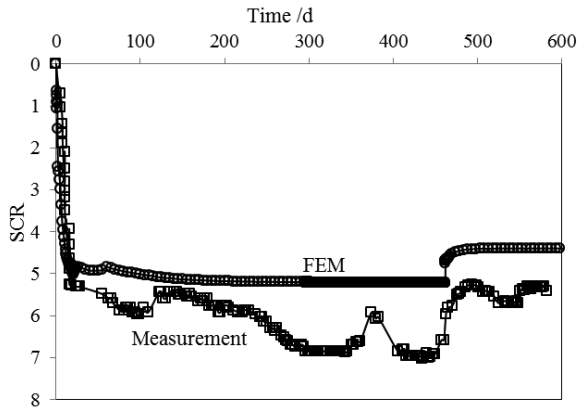


**Figure 6**. Development of the stress-concentration ratios (SCR).

### 3.2.5 Axial force of the pile

Fig. 7 shows the distribution of the axial load along the length of the pile. As is clear from the figure, the axial load was firstly increased, while it decreased after a certain depth, and the reduction ratio increased when near the bottom of the pile. This may due to the negative frictional stress existing along the pile. The results of the FEM showed a similar trend to the measurement, while they were underestimated at the top of the pile. This was consistent with the comparison of the SCR, in which the SCR from the FEM was underestimated. Less stress acting on the pile cap would result in a smaller axial force in the pile.

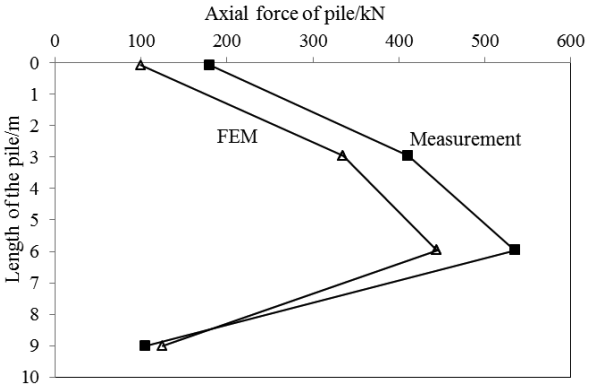


**Figure 7**. Axial force of the pile.

### 3.2.6 Frictional stress along the pile

The frictional stress was generated due to the differential settlement between the piles and the surrounding soil. The negative frictional stress will be generated when the settlement of the piles was larger than that of the subsoil. In contrast, a positive frictional stress occurred. Hence, a neutral point will be generated when the settlement of the pile equals that of the subsoil, which was approximately 6.8 m depth of the pile in Fig. 8. Since the frictional stress was derived from the axial force of the pile, the comparison of the FEM and the measurement was therefore similar to that of the axial force of the pile. The negative frictional stress was underestimated by the FEM, while it was overestimated for the positive frictional stress.

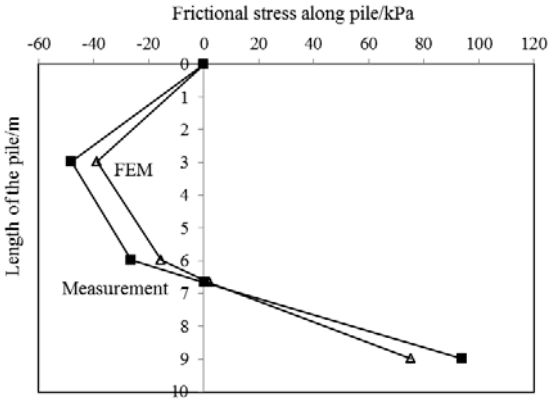


**Figure 8**. Frictional stress along the pile.

As illustrated above, the results of the FEM and the measurement showed a closer agreement. The FEM gave almost the same results to that of the field measurements in terms of the settlement, but with a slight difference. The stress-concentration ratio (SCR), the axial force and the frictional stress were somehow underestimated by the FEM. The settlement of the subsoil from the FEM was therefore a reliable parameter to assess the performance of the pile embankment.

## 4. ANALYTICAL METHODS

The stress-concentration ratio (SCR) predicted by the modified Terzaghi method (Russell and Pierpoint, 1997) [4] will be presented in the paper, together with the settlement of the subsoil at the centerline of the embankment and the tensile force of the geosynthetic reinforcement by Zhuang et al. (2014) [10].

### 4.1 Stress-concentration ratio

Terzaghi (1943) [3] proposed an analytical solution based on the trapdoor experiment. Two vertical shear planes were assumed to occur in the soil as the trapdoor descended and the shear stress applied to the soil mass, directly above the trapdoor, the shear stress decreased the soil pressure on the trapdoor and increased the pressure on the adjoining stationary soil mass. It was reported by Russell and Pierpoint (1997) [4] that for the three-dimensional condition, the stress-reduction ratio (SRR) could be expressed as follows:

$$SRR = \frac{\left(s^2 - a^2\right)}{4haK\tan\varphi}\left(1 - e^{\frac{-4haK\tan\varphi}{(s^2-a^2)}}\right) \qquad (4)$$

Based on the equilibrium equation for the vertical force at the bottom of the embankment, the SCR can be derived as follows:

$$SCR = \frac{s^2 - SRR(s^2 - a^2)}{SRR\,a^2} \qquad (5)$$

where $K$ is the empirical constant, and can be taken as 0.7, according to Terzaghi (1943) [3] and Chen et al.(2008) [16]; $h$ is the height of the embankment; $s$ is the pile spacing between piles; $a$ is the width of the pile cap; and $\varphi$ is the effective friction angle of the embankment.

### 4.2 Settlement of the subsoil at the centerline of the embankment

Zhuang et al. (2014) [10] proposed an analytical model to evaluate the maximum settlement at the surface of the subsoil and the maximum strain of the geogrid. For the reinforced, piled embankment, taking the unit body immediately below the reinforcement between the pile caps, the vertical equilibrium required that:

$$\frac{64k_g}{3l^4}\delta^3 + E_0\frac{\delta}{h_s} - \sigma_G = 0 \qquad (6)$$

where $k_g$ is the tensile stiffness of the reinforcement; $l$ is the span of the tensile reinforcement, and is taken as $(s\text{-}a)\ (1+\sqrt{2})/2$; $\delta$ is the maximum settlement at the surface of the subsoil; $h_s$ is the thickness of subsoil; $E_0$ is the one-dimensional stiffness, which can be derived from

the Young's modulus and the Poisson's ratio; and $\sigma_G$ is the vertical stress at the base of the embankment, including the action of arching. The maximum settlement of the subsoil can be obtained by solving Equation 6.

### 4.3 Maximum tensile force in the reinforcement

The maximum tensile force ($T$) in the reinforcement can be expressed in terms of the maximum settlement at the surface of the subsoil, as follows:

$$T = k_g \frac{8\delta^2}{3l^2} \qquad (7)$$

### 4.4 Comparison of the results from the analytical method, the FEM and the measurements

Fig. 9 shows the results of the comparison in terms of the SCR between the analytical method, the FEM and the measurements. As is clear from Fig. 9, the SCR predicted by the modified Terzaghi method increased with an increase in the embankment height $h$, which implied that more vertical stress was transferred onto the pile cap with an increase in the embankment height. The SCR from the modified Terzaghi method was overestimated, with a value of approximately 25%, while it was underestimated by the FEM, with a value of 20%. It showed that the modified Terzaghi method was more conservative in terms of the SCR than that of the FEM. It was also shown that the SCR was not a reliable parameter when assessing the performance of the embankment.

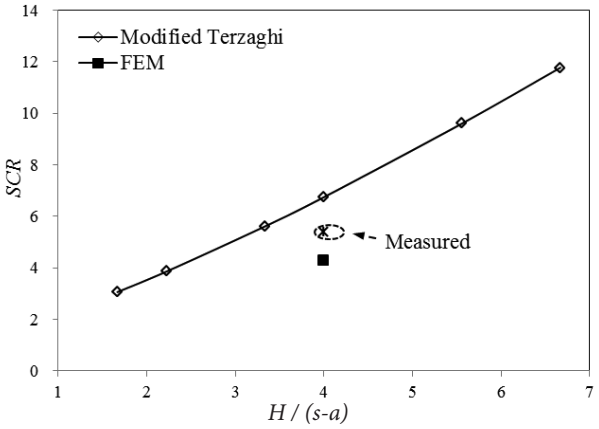


**Figure 9**. Comparison of SCR with the analytical method, the FEM and the measurement.

The results of the comparison for the maximum settlement of subsoil ($\delta$) are presented in Fig. 10. The maximum settlement of the subsoil increased with an increase in the embankment height, and was slightly overestimated, with a value of 5%, while the results from the FEM were underestimated, with the value of 8.2%. Both the

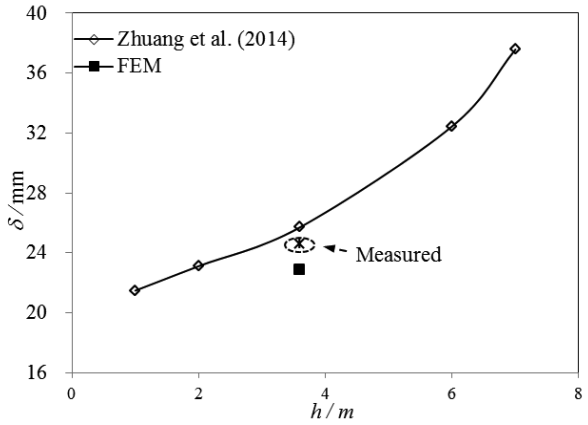


**Figure 10**. Comparison of the maximum settlement of subsoil with the analytical method, the FEM and the measurement.

analytical method of Zhuang et al. (2014) [10] and the FEM showed reasonable agreement with the measurement. The maximum settlement of the subsoil was therefore a reliable parameter to evaluate the performance of the piled embankment with reasonable accuracy.

As shown in Fig. 11, a comparison of the maximum tensile force in the reinforcement was presented. The maximum tensile force in the reinforcement also increased with an increase of the embankment height, and was slightly overestimated, with a value of less than 7%. The results predicted by the FEM were also overestimated; however, with a value of approximately 44%. The tensile force can therefore be assessed using the analytical method presented in Zhuang et al. (2014) [10] with reasonable accuracy, while the results of the FEM were much more conservative.

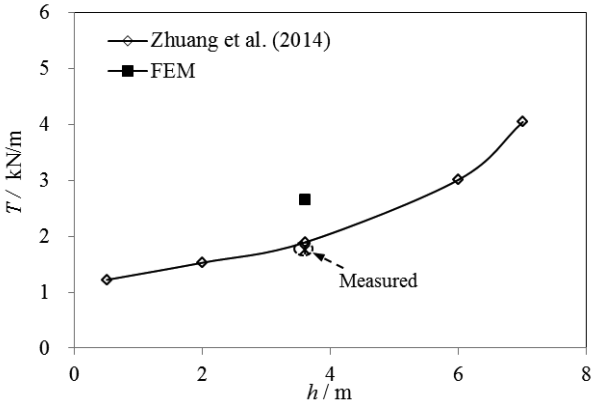


**Figure 11**. Comparison of the maximum tensile force in the reinforcement with the analytical method, the FEM and the measurement.

## 5 CONCLUSIONS

A full-scale field case of the Fengyang high-speed railway was presented in this paper, in which the embank-

ment was constructed over soft soil, and was improved by the combined use of the CFG pile-net composited foundation and preloading. Numerous devices were used to monitor the evaluation of the embankment. Numerical simulations and analytical methods were used to predict the behavior of the embankment.

The results of the numerical simulation were compared with the measurements, in terms of the development for the settlement of subsoil at the centerline of the embankment, the distribution of the settlement of subsoil along the width of the embankment, the lateral deformation of the subsoil, the stress/concentration ratio (SCR), the axial force of the pile and the frictional stress along the pile. It showed that the results of the FEM were in good agreement with the measurements. It was also shown that the SCR was underestimated by the FEM, as well as the axial force and the frictional stress of the pile.

The comparison of the analytical methods with the FEM results and the measurements also showed that the settlement of the subsoil was a reliable parameter to assess the performance of the embankment with reasonable accuracy. The SCR predicted by the modified Terzaghi method was overestimated, with a difference of 25%, while it was underestimated by the FEM, with a difference of 20%. It was also shown that the tensile force in the reinforcement can be effectively assessed by Zhuang et al. (2014) [10], while it was overestimated by the FEM, with the amount being conservative.

## Acknowledgements

The financial support of the National Natural Science Foundation of China (Grant No. 51478166 and 51108155), the Fundamental Research Funds for the Central Universities (Grant No. 2015B06014 and 2015B17814) and the Scientific Research Foundation for the Returned Overseas Chinese Scholars, State Education Ministry, is acknowledged.

## REFERENCES

[1] Magnan, J.P., 1994. Methods to reduce the settlement of embankments on soft clay: A review. Vertical and Horizontal Deformations of Foundations and Embankments. ASCE Geotechnical Special Publication 1, 40, 77-91.

[2] Gangakhedkar R. 2004. Geosynthetic reinforced pile supported embankments. Master thesis, University of Florida.

[3] Terzahgi, K. 1943. Theoretical Soil Mechanics. John Wiley and Sons, New York.

[4] Russell, D., Pierpoint, N. 1997. An assessment of design methods for piled embankments. Ground Engineering 30, 10, 39-44.

[5] Hewlett, W.J., Randolph, M.F. 1988. Analysis of piled embankments. Ground Engineering 21, 3, 12-18.

[6] BS8006-1, 2010. Code of practice for strengthened/reinforced soils and other fills. British Standards Institution, UK.

[7] EBGEO, 2011. Recommendations for Design and Analysis of Earth Structures using Geosynthetic Reinforcements EBGEO, 2011. ISBN 978-3-433-02983-1 and digital in English ISBN 978-3-433-60093-1.

[8] Kempfert, H.G., Göbel, C., Alexiew, D., Heitz, C. 2004. German recommendations for reinforced embankments on pile-similar elements. In Euro-Geo3-Third European Geosynthetics Conference, Geotechnical Engineering with Geosynthetics, pp. 279-284.

[9] Van Eekelen, S.J.M., Bezuijen, A. and Van Tol, A.F. 2011. Analysis and modification of the British Standard BS8006 for the design of piled embankments. Geotextiles and Geomembranes 29, 3, 345-359.

[10] Zhuang,Y., Wang, K.Y., Liu, H.L. 2014. A simplified model to analyze the reinforced piled embankment. Geotextiles and Geomembranes 42, 2, 154-165.

[11] Han, J., Gabr, M. A. 2002. Numerical analysis of geosynthetic reinforced and pile-supported earth platforms over soft soil. Journal of Geotechnical and Geoenvironmental Engineering 128, 1, 44-53.

[12] Le Hello, B., Villard, P. 2009. Embankments reinforced by piles and geosynthetics numerical and experimental studies with the transfer of load on the soil embankment. Engineering Geology 106, 1-2, 78-91.

[13] Zeng, J.C. 2010. Experiment study and theoretical analysis of CFG pile composite foundation in high-speed railway. PhD thesis, Southeast University, China (In Chinese)

[14] Liu, H. L., Charles, W. W., Fei, K. 2007. Performance of a Geogrid-Reinforced and Pile-Supported Highway Embankment over Soft Clay: Case Study. ASCE, Journal of Geotechnical and Geoenvironmental Engineering 133, 1483-1493.

[15] Potyondy J.G. 1961. Skin friction between various soils and construction materials. Geotechnique 11, 4, 339-353.

[16] Chen, Y.M., Cao, W.P., Chen, R.P. 2008. An experimental investigation of soil arching within basal reinforced and unreinforced piled embankments. Geotextiles and Geomembranes 26, 2, 164-174.